

## MAGNETIC PROPERTIES OF HIGH PETROLOGIC GRADE L-LL CHONDRITES: TENHAM, TUXTUAC, WILLARD AND FORREST(b)

Atsuko YAMANAKA<sup>1</sup>, Minoru FUNAKI<sup>2</sup> and Hiroyuki NAGAI<sup>1</sup>

<sup>1</sup>*Department of Physics, Faculty of Science, Shinshu University,  
1-1, Asahi 3-chome, Matsumoto 390*

<sup>2</sup>*National Institute of Polar Research, 9-10, Kaga 1-chome,  
Itabashi-ku, Tokyo 173*

**Abstract:** Temperature dependence of the hysteresis parameters (saturation magnetization,  $J_s$ ; saturation remanent magnetization,  $J_r$ ; coercivity,  $H_c$ ; and initial susceptibility,  $X_i$ ) were examined from room temperature to 780°C for Tenham (L6), Tuxtuac (LL5), Willard (L6) and Forrest(b) (L6) chondrites. Their main magnetic minerals were determined from the analyses of transition temperatures ( $\Theta_{J_s}$ ,  $\Theta_{H_c}$ ,  $\Theta_{X_i}$ ). The NRM characteristics of these chondrites were measured and are discussed on the basis of magnetic properties. The main magnetic minerals of the Tenham chondrite are taenite ( $\gamma$ -(Fe, Ni)) with 54 at% Ni and kamacite ( $\alpha$ -(Fe, Ni)) with 7 at% Ni, and the main NRM carrier is taenite. Tenham has a stable NRM. Tuxtuac mainly contains tetrataenite and taenite (the ratio tetrataenite : taenite is 15:85, T. NAGATA *et al.*, Mem. Natl Inst. Polar Res., Spec. Issue, **41**, 364, 1986) and they both contribute to NRM. The NRM of Tuxtuac is rather unstable magnetically. The main magnetic minerals of the Willard chondrite are the same as those of Tenham, i.e. taenite with 54 at% Ni and kamacite with 7 at% Ni. The main NRM carrier is taenite. Willard has an unstable NRM. Forrest is suggested to have experienced some alteration, on the basis of the analysis of the  $J_s$ - $T$  curve, and may have acquired a secondary NRM of probable terrestrial origin.

### 1. Introduction

The magnetic properties of meteorites containing tetrataenite have been reported by NAGATA and FUNAKI (1982, 1987), NAGATA *et al.* (1986, 1987), and WASILEWSKI (1982, 1985); and the temperature dependent behavior of the magnetic coercivity of meteorites containing tetrataenite has been reported by FUNAKI (1993). Tetrataenite or ordered FeNi with a tetragonal super lattice was first discovered by ALBERTSEN *et al.* (1978). The tetrataenite is expected to carry a stable NRM because of the uniaxial character and the large magnetocrystalline anisotropy value reported by NÉEL *et al.* (1964).

Magnetic properties of bulk samples of ordinary chondrites are due to kamacite, taenite, tetrataenite and/or plessite and other ferromagnetic minerals. Chondrites classified as a high petrologic type have the possibility to have acquired the TRM (or thermally blocked NRM) if their parent bodies had possessed a magnetic field during their cooling process, because they seem to have been heated to higher temperatures than the Curie points of the above-mentioned magnetic minerals. If the tetrataenite

expected to carry the stable NRM is contained in a chondrite, and its parent body had possessed a magnetic field, it has a possibility to have acquired CRM (chemical remanent magnetization) when the tetrataenite was formed.

Three L chondrites, Tenham, Willard and Forrest(b), and one LL chondrite, Tuxtuac, of high petrologic type were studied in the present study. It has been reported by NAGATA *et al.* (1986) that Tuxtuac contains tetrataenite.

## 2. Samples and Experiments

Subsamples (about 0.1 g) were obtained from the interior of Tenham(L6), Tuxtuac(LL5), Willard(L6) and Forrest(b)(L6). Their magnetic hysteresis loops between  $-1.0$  and  $+1.0$  T external magnetic field were obtained using a VSM (vibrating sample magnetometer). It took 20 min to measure a complete loop. The samples were heated from room temperature to  $780^{\circ}\text{C}$  and cooled at the rate  $50^{\circ}\text{C/h}$  in a  $10^{-5}$  Torr vacuum. The hysteresis properties, or  $J_s$ ,  $J_r$ ,  $H_c$  and  $X_i$  values, were determined from the loop. The hysteresis loops of the powder samples (about 0.1 g) of the magnetic fractions obtained from each chondrite by hand magnetic separation were also measured by the same procedure as the bulk samples.

Six small samples (0.05 g on average) were obtained from each chondrite. The NRM characteristics of the three small samples were examined against thermal demagnetization every  $50^{\circ}\text{C}$  from  $180^{\circ}\text{C}$  to  $630^{\circ}\text{C}$ , and those of the other three small samples were examined against AF demagnetization at every 5 mT up to 50 mT. During the thermal demagnetization, samples were in the vacuum condition of  $10^{-4}$  Torr. The NRM was measured by the SQUID magnetometer during thermal demagnetization, and the spinner magnetometer during AF demagnetization.

The NRM of a cubic sample (2.5 g on average) obtained from each chondrite was measured. The cube was cut into eight small cubes and the small cubes were oriented mutually. The intensities and directions of their NRMs were measured using the spinner magnetometer.

## 3. Experimental Results

### 3.1. Tenham

#### 3.1.1. Thermomagnetic analysis

The  $J_s$ - $T$  curve of bulk sample of Tenham (Fig. 1a) showed apparent transition points ( $\Theta_{J_s}$ ) at  $590^{\circ}\text{C}$  and at  $770^{\circ}\text{C}$  on the heating curve and at  $660^{\circ}\text{C}$  on the cooling curve. There were also two minor transition points at  $540^{\circ}\text{C}$  on the heating curve and  $\Theta_{J_s}$  at  $590^{\circ}\text{C}$  on the cooling curve (Table 2). The  $J_s=7.75$  Am<sup>2</sup>/kg of the original sample increased to  $J_s=9.70$  Am<sup>2</sup>/kg after heating to  $780^{\circ}\text{C}$  due to oxidation of sulfide (FUNAKI, 1993) (Table 1) and/or FeOOH.

On the other hand, the  $J_s$ - $T$  curve of the magnetic fraction obtained by hand magnetic separation (Fig. 1b) showed  $\Theta_{J_s}$  at  $580^{\circ}\text{C}$  and at  $750^{\circ}\text{C}$  on the heating curve and  $\Theta_{J_s}$  at  $630^{\circ}\text{C}$  on the cooling curve. (There was a minor  $\Theta_{J_s}$  at  $260^{\circ}\text{C}$  on the heating curve.) The  $J_s=49.6$  Am<sup>2</sup>/kg at  $30^{\circ}\text{C}$  hardly changed after heating to  $780^{\circ}\text{C}$  (Table 1). The main magnetic minerals of the Tenham meteorite are  $\gamma$ -(Fe, Ni) or taenite with

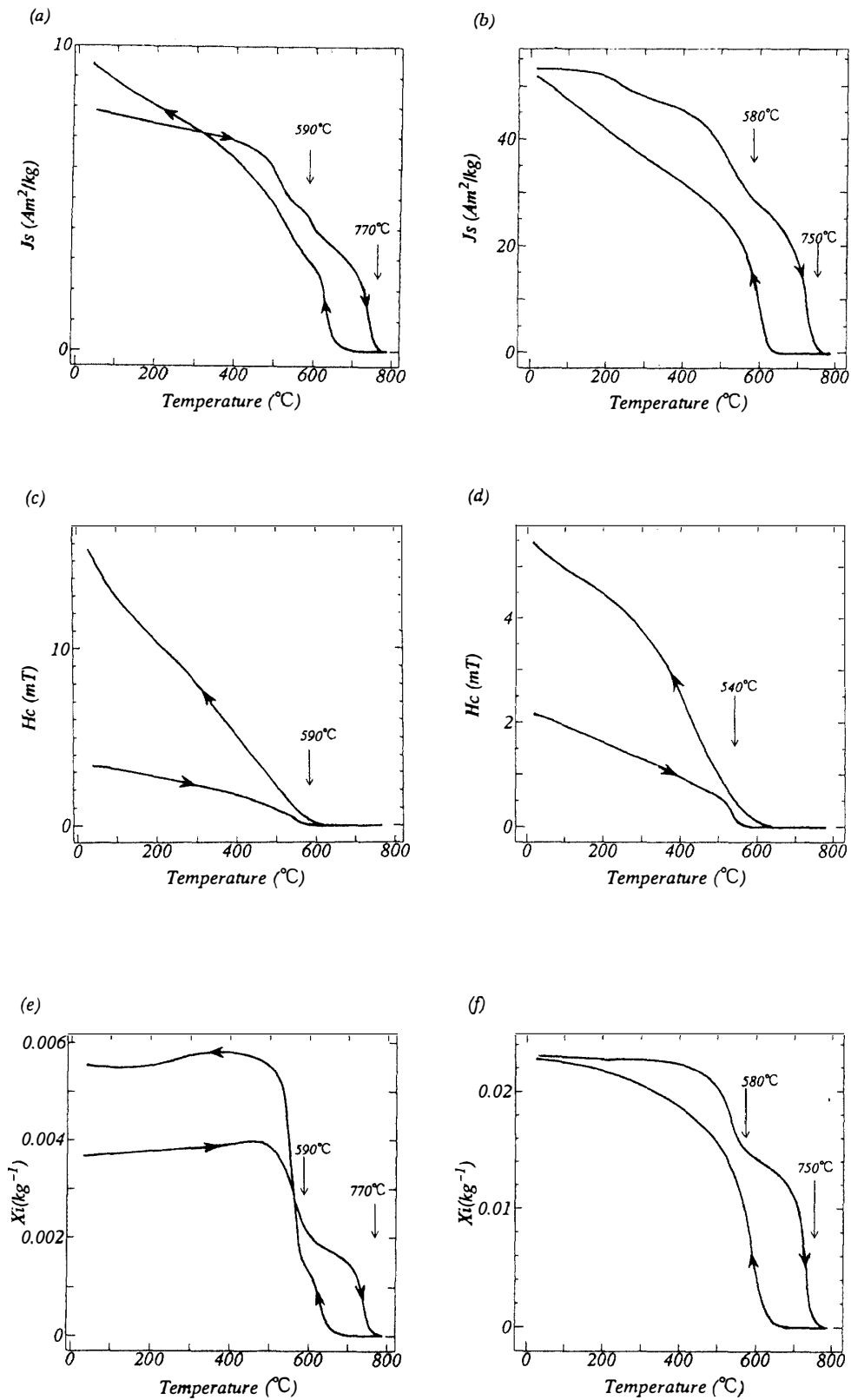


Fig. 1. Temperature dependence of  $J_s$ ,  $H_c$ ,  $\chi_i$  values for Tenham chondrite. (a)(c)(e):  $J_s$ ,  $H_c$ ,  $\chi_i$  of the bulk sample. (b)(d)(f):  $J_s$ ,  $H_c$ ,  $\chi_i$  of the magnetic fraction (powder).

54 at% Ni ( $\Theta_{Js}$  at 580°–590°C as the apparent Curie point) and  $\alpha$ -(Fe, Ni) or kamacite with 6 at% Ni on average ( $\Theta_{Js}$  at 750°–770°C as the  $\alpha$ - $\gamma$  transformation temperature).

The  $Hc$ - $T$  curve of the bulk sample (Fig. 1c) showed  $\Theta_{Hc}$  at 560°C on the heating curve and  $\Theta_{Hc}$  at 590°C on the cooling curve. The kamacite had no coercivity above 550°C on the heating curve or above 590°C on the cooling curve. The initial  $Hc=3.45$  mT (Table 1) increased to 15.22 mT after heating to 780°C. There was no evidence of  $\gamma'$ -(Fe, Ni) or tetrataenite. The  $Hc$ - $T$  curve of the magnetic fraction showed  $\Theta_{Hc}$  at 540°C on the heating curve and  $\Theta_{Hc}$  or 590°C on the cooling curve (Fig. 1d). The  $Hc=2.08$  mT changed to 5.05 mT and the ratio of  $Hc$  (after) to  $Hc$  (before) for the magnetic fraction was smaller than that of the bulk sample (Table 1).

The  $Xi$ - $T$  curve of the bulk sample, as shown in Fig. 1e, increased slightly (1%) up to 480°C and then abruptly decayed between 480°C and  $\Theta_{Xi}$  at 590°C; the  $Xi$  disappeared at  $\Theta_{Xi}$  at 770°C on the heating curve. On the cooling  $Xi$ - $T$  curve there are  $\Theta_{Xi}$  at 660°C and 590°C. Below  $\Theta_{Xi}$  at 660°C the  $Xi$  increased abruptly to 520°C and then decreased very slightly to room temperature on the cooling curve. The original  $Xi=3.69 \times 10^{-3}$  increased to  $Xi=5.64 \times 10^{-3}$  after heating to 780°C (Table 1). The  $Xi$  of the magnetic fraction hardly changed up to 480°C and decreased abruptly between 480°C and  $\Theta_{Xi}$  at 580°C and then reached 0 through  $\Theta_{Xi}$  at 750°C on the heating curve. The cooling  $Xi$ - $T$  curve showed an apparent  $\Theta_{Xi}$  at 630°C and a minor  $\Theta_{Xi}$  at 580°C (Fig. 1f). The original  $Xi=2.09 \times 10^{-2}$  hardly changed after heating to 780°C

Table 1. Basic data of hysteresis parameters at room temperature (no-mak: original, \*: after heated) and REM (the ratio of NRM to saturation remanence) range of bulk subsamples (n: number of subsamples measured NRM and calculated REM).

Meteorite	Treatment unit	$J_s$ (Am <sup>2</sup> /kg)	$J_r$ (Am <sup>2</sup> /kg)	$H_c$ (mT)	$Xi \times 10^{-3}$ (kg <sup>-1</sup> )	REM (NRM/ $J_r$ ) range
Tenham	bulk	7.75 *9.70	0.13 *0.86	3.45 *15.22	3.69 *5.64	0.0031 
	magnetic powder	49.60 *50.30	0.44 *0.91	2.08 *5.05	20.9 *23.4	0.051 (n=13)
Tuxtuac	bulk	0.20 *0.48	0.03 *1.01	37.78 *23.16	0.09 *4.37	0.096 
	magnetic powder	62.9 *67.9	0.83 *0.71	3.61 *2.79	23.0 *25.9	0.23 (n=13)
Willard	bulk	3.76 *5.06	0.63 *1.31	10.18 *18.04	5.12 *7.80	0.0032 
	magnetic powder	13.01 *14.20	1.31 *2.60	5.88 *10.28	22.05 *23.56	0.27 (n=23)
Forrest	bulk	5.86 *6.21	1.40 *1.19	23.80 *25.24	5.87 *7.84	0.00033 
	magnetic powder	22.00 *27.00	1.18 *3.00	6.40 *19.72	37.9 *30.9	0.047 (n=13)

Table 2. Basic data of the temperature dependence of hysteresis parameters.

Meteorite	Treatment unit	$\Theta_{Js}$ (°C)	$\Theta_{Hc}$ (°C)	$\Theta_{Xi}$ (°C)
Tenham	bulk <sub>(original)</sub>	540 590 770	560	590 770
	(heated)	590 660	590	590 660
	magnetic <sub>(o)</sub>	260 580 750	540	580 750
	powder <sub>(h)</sub>	630	590	580 630
Tuxtuac	bulk <sub>(original)</sub>	—	—	—
	(heated)	—	—	—
	magnetic <sub>(o)</sub>	320 520	200 320 460 540	520 580
powder <sub>(h)</sub>	590	280 580	600	
Willard	bulk <sub>(original)</sub>	200 580 730	200 410 550	580 730
	(heated)	630	600	640
	magnetic <sub>(o)</sub>	580 730	200 550	580 730
	powder <sub>(h)</sub>	630	430 580	580 630
Forrest	bulk <sub>(original)</sub>	300 400 590 760	300 540	360 590 760
	(heated)	410 580	540 580	580
	magnetic <sub>(o)</sub>	560 720	410 540	580 720
	powder <sub>(h)</sub>	520 600	340 580	620

(Table 1).

### 3.1.2. Natural remanent magnetization

NRM directions of eight small cubes are well grouped (Fig. 2). Intensity and direction of the remaining NRM of Tenham meteorite in course of stepwise thermal demagnetization from 180°C to 630°C, at temperature intervals of 50°C, are shown in Fig. 3a. The subsample characteristics of Tenham's NRM during thermal demagnetization seem to be uniform in Fig. 3a1. Tenham loses NRM completely above 580°C, due to disappearance of coercivity (Fig. 1c). It seems that the main NRM carrier of

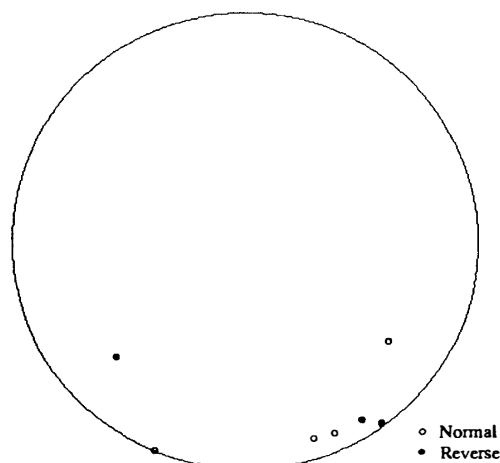


Fig. 2. NRM directions of eight small cubes obtained from Tenham.

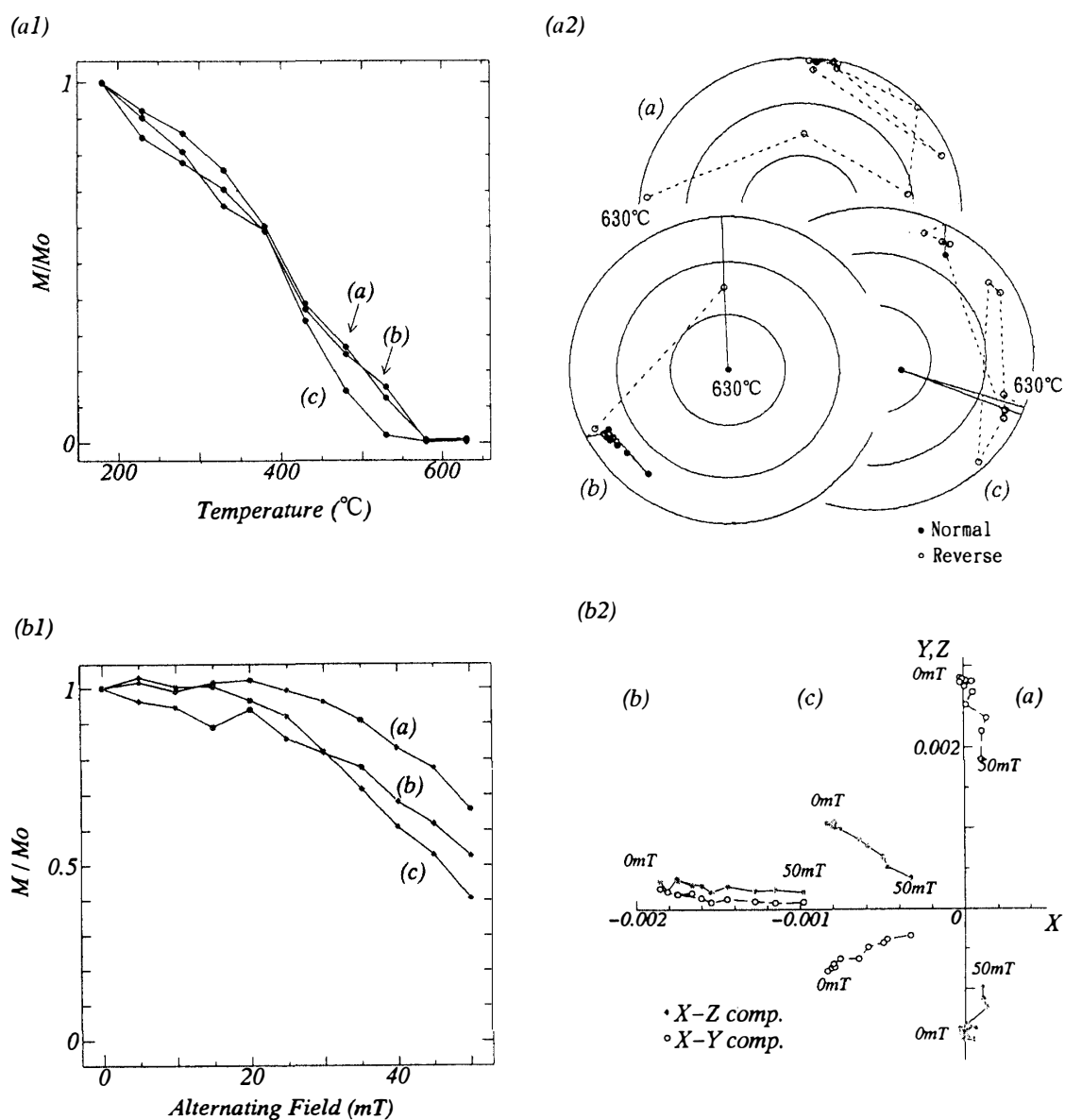


Fig. 3. Characteristics of NRM of Tenham against thermal and AF demagnetization. (a1) Intensity changes against thermal demagnetization. (a2) Directional changes against thermal demagnetization. (b1) Intensity changes against AF demagnetization. (b2) Directional changes against AF demagnetization.

Tenham is taenite and the contribution of abundant kamacite to Tenham's NRM is small. Directional changes of residual NRM against thermal demagnetization, shown in Fig. 3a2, had no apparent stable pattern among the three subsamples of Tenham. It seems that the NRM of Tenham had not been thermally blocked in its parent body.

Results of AF demagnetization are shown in Fig. 3b. The NRM of Tenham was very stable against AF demagnetization; 40–70% of the intensity of the original NRM remained up to 50 mT (Fig. 3b1). The changes of direction of NRM against AF demagnetization (shown in the Zijderveld projection—Fig. 3b2) are relatively small

and the NRM seems to consist of one component. The coercivity carried by magnetic grains in Tenham seems to be distributed uniformly and be stable.

### 3.2. Tuxtuac

#### 3.2.1. Thermomagnetic analysis

NAGATA *et al.* (1986) reported the average composition of metals in Tuxtuac, determined by Mössbauer spectrum analysis, to be (tetrataenite) : (disorder taenite) : (kamacite)=15:85:( $\leq 0$ ) in wt%. Figure 4 shows the hysteresis loops before and after heating, to 780°C, for a bulk sample of Tuxtuac measured at room temperature. The sample was not saturated at 1 T for high coercivity, related to anisotropy, but after heating it was saturated for small coercivity. The original hysteresis loop (Fig. 4a) showed quite small magnetic initial susceptibility and high coercivity. The  $X_i=9.25 \times 10^{-5}$  before heating increased to  $X_i=4.37 \times 10^{-3}$  after heating; the  $H_c=37.78$  mT before heating decreased to  $H_c=23.16$  mT after heating to 780°C (Table 1). This is identical to the magnetic properties of the tetrataenite (NAGATA *et al.*, 1987) and disordering, or transformation, of the tetrataenite to ordinary taenite (SCORZELLI and DANON, 1985).

On the other hand, results of magnetic fraction obtained by hand magnetic separation from Tuxtuac are shown in Fig. 5. The  $J_s$ - $T$  curve (Fig. 5a) showed  $\Theta_{J_s}$  at 520°C on the heating curve and  $\Theta_{J_s}$  at 590°C on the cooling curve. (There were also minor  $\Theta_{J_s}$  at 320°C on the heating curve.) The kamacite was absent in Tuxtuac. The  $J_s=6.29 \times 10$  Am<sup>2</sup>/kg at room temperature before heating increased to  $J_s=6.79 \times 10$  Am<sup>2</sup>/kg very slightly (Table 1). The  $H_c$  increased gradually from room temperature to 400°C and then decreased abruptly between 500°C and 550°C on the heating curve (Fig. 5b). The course of increase would seem to indicate that FeOOH (as a weathering product) was altered to Fe<sub>3</sub>O<sub>4</sub> gradually by heating in the  $10^{-5}$  Torr vacuum. After heating to 780°C the  $H_c$  appeared through the  $\Theta_{H_c}$  at 580°C and increased abruptly till 500°C, and then increased gradually through the minor  $\Theta_{H_c}$  at 280°C. The pre-heating coercivity  $H_c=3.61$  mT decreased to 2.79 mT after heating

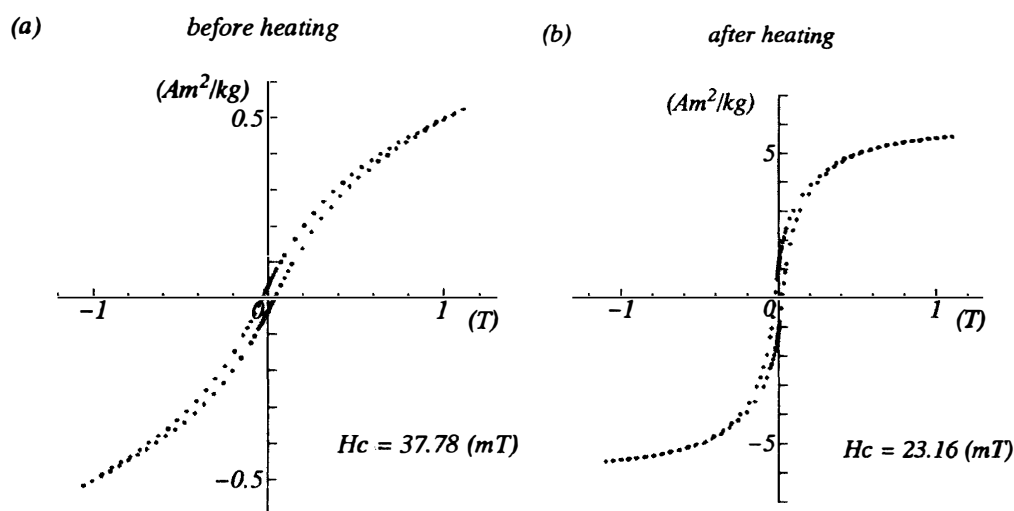


Fig. 4. Hysteresis loops of Tuxtuac chondrite of (a): before heating and (b): after heating.

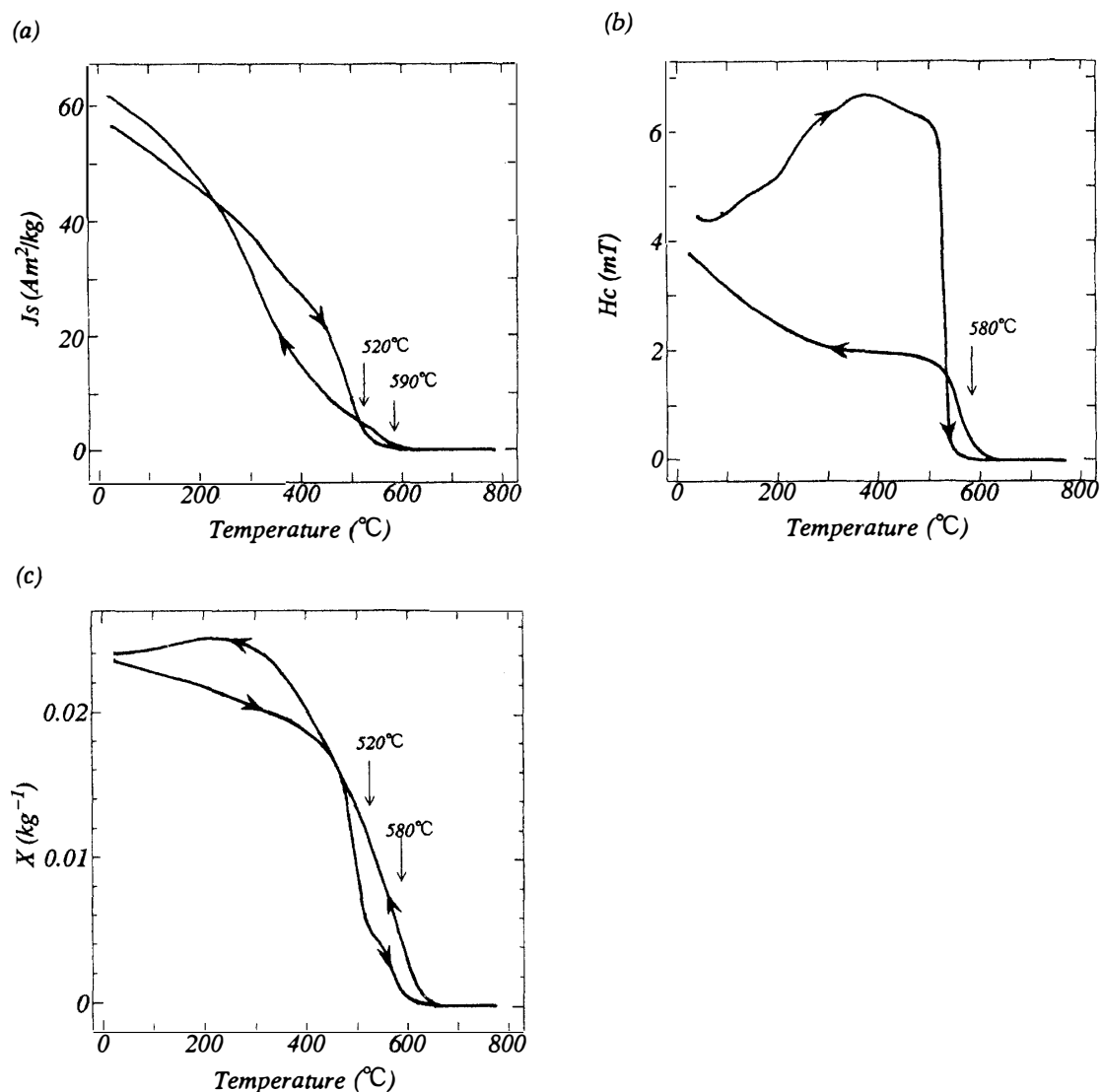


Fig. 5. Temperature dependence of (a):  $J_s$ , (b):  $H_c$ , (c):  $X_i$  values for the magnetic fraction (powder) of Tuxtuac.

(Table 1). The  $X_i$ - $T$  curve of the magnetic fraction of Tuxtuac is shown in Fig. 5c. The heating  $X_i$ - $T$  curve showed major  $\Theta_{X_i}$  at 580°C and minor  $\Theta_{X_i}$  at 520°C. The cooling  $X_i$ - $T$  curve showed a major  $\Theta_{X_i}$  at 600°C. The  $X_i = 2.30 \times 10^{-2}$  before heating increased to  $X_i = 2.59 \times 10^{-2}$  very slightly after heating to 780°C (Table 1).

### 3.2.2. Natural remanent magnetization

NRM directions of eight small cubes obtained from Tuxtuac were reasonably well grouped (Fig. 6). NRM of the bulk samples of Tuxtuac meteorite was thermally demagnetized, in steps of 50°C, from 180°C to 630°C. Thermal demagnetization curves of NRM intensities for three subsamples showed very similar characteristics, as shown in Fig. 7a1; they showed a curve of a constant gradient up to 480°C and then an abrupt decrease to 530°C. Significant residual remanence was not observed above 530°C. The changes of directions were clustered within one direction with 20 to 40

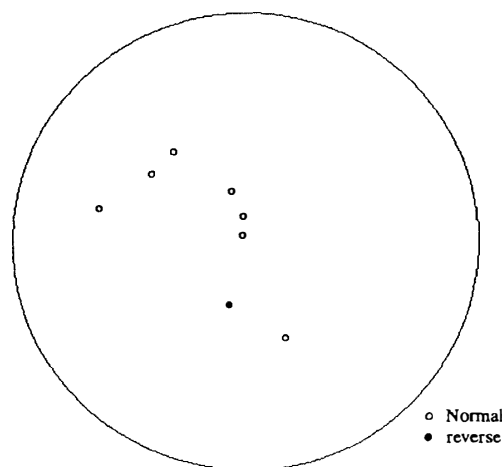


Fig. 6. NRM directions of eight small cubes of Tuxtuac.

degrees scatter up to 480°C (Fig. 7a2) and then showed a larger shift above 530°C.

Results of AF demagnetization are shown in Fig. 7b. Original NRM intensities of bulk samples of Tuxtuac were 70–98%, demagnetized by 25 mT (Fig. 7b1). The NRM directions in Fig. 7b2 show two components of NRM except the IRM demagnetized at 5 mT; the lower coercivity component dominated between 0 to 10 mT and the higher coercivity component from 10 or 15 mT. The NRM of Tuxtuac showed very soft characteristics against the alternating field.

### 3.3. Willard

#### 3.3.1. Thermomagnetic analysis

The  $J_s$ - $T$  curve of Willard meteorite (Fig. 8a) had clearly defined transition points, or  $\Theta_{J_s}$ , at 580° and 730°C on the heating curve and  $\Theta_{J_s}$  at 630°C on the cooling curve. (It showed a minor  $\Theta_{J_s}$  at 200°C on the cooling curve). The  $J_s=3.76$  Am<sup>2</sup>/kg of the original sample increased to  $J_s=5.06$  Am<sup>2</sup>/kg after heating to 780°C. The  $J_s$ - $T$  curve of the magnetic fraction obtained by hand magnetic separation (Fig. 8b) showed transition points the same as those of the bulk sample. The main magnetic minerals of Willard meteorite are taenite with 54 at% Ni ( $\Theta_{J_s}$  at 580°C as the apparent Curie point) and kamacite with 7 at% Ni ( $\Theta_{J_s}$  at 730°C as the  $\alpha$ - $\gamma$  transformation temperature).

The  $H_c$ - $T$  curve (Fig. 8c) showed an apparent  $\Theta_{H_c}$  at 550°C and a minor  $\Theta_{H_c}$  at 410°C upon heating. The original  $H_c=10.18$  mT increased to  $H_c=18.04$  mT, measured at room temperature, after heating (Table 1). The  $H_c$ - $T$  curve of the magnetic component powder showed the  $\Theta_{H_c}$  at 550°C on the heating curve and the  $\Theta_{H_c}$  at 580°C on the cooling curve. The abundant kamacite in Willard had no significant coercivity between 550°C and its transformation point to paramagnetic taenite at 730°C.

The  $X_i$  of the original sample increased gradually from room temperature to 500°C and then abruptly decreased in the range 550°–580°C (Fig. 8e). It decreased slightly between 580° and 700°C and then disappeared through the apparent  $\Theta_{X_i}$  at 730°C. The  $X_i$  increased abruptly between  $\Theta_{X_i}$  at 630°C and 500°C and showed a

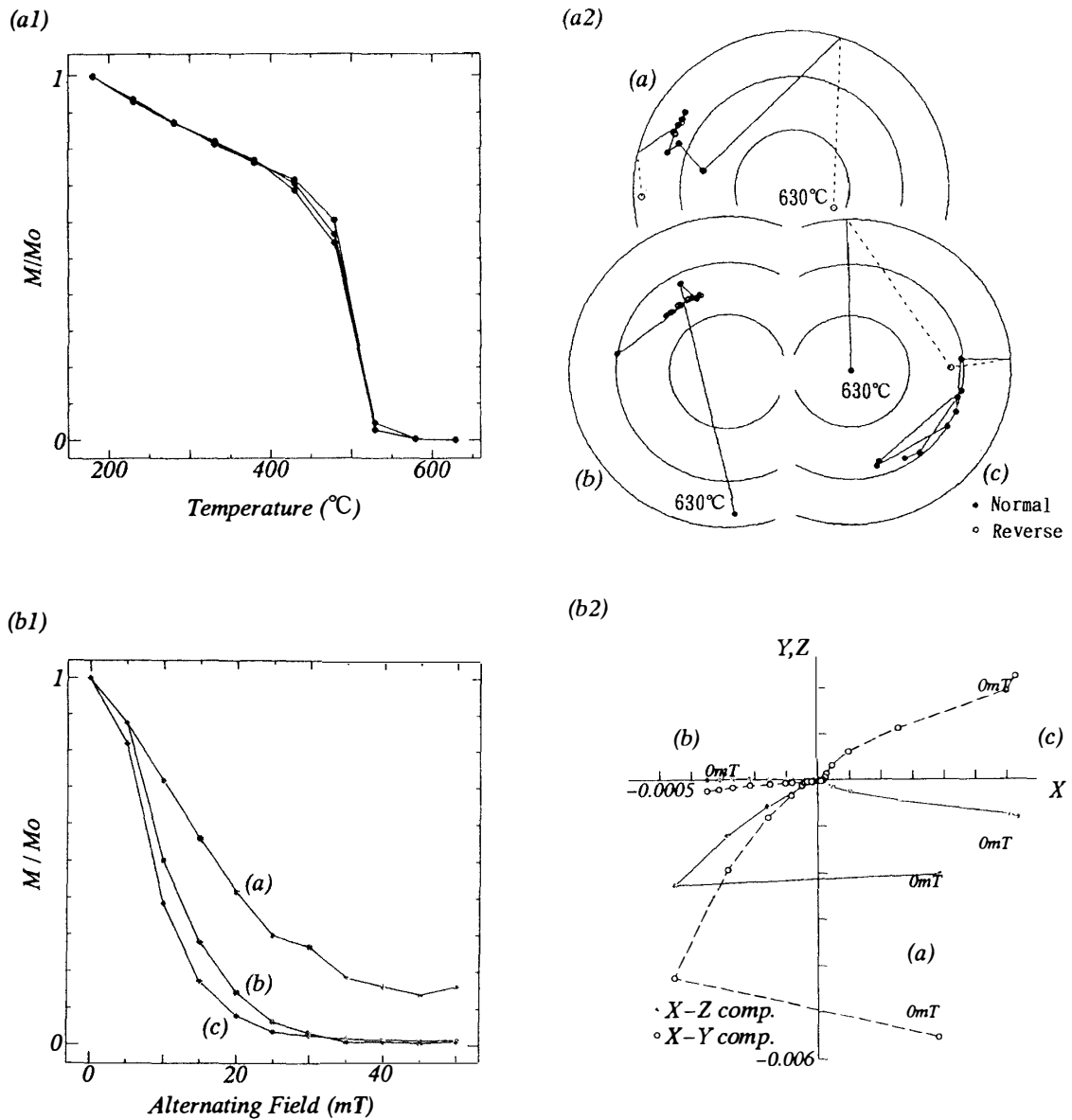


Fig. 7. Characteristics of NRM of Tuxtuac against thermal and AF demagnetization. (a1) Intensity changes against thermal demagnetization. (a2) Directional changes against thermal demagnetization. (b1) Intensity changes against AF demagnetization. (b2) Directional changes against AF demagnetization.

maximum at 500°C; then it decreased through a concave point at 320°C. The original  $X_i = 5.12 \times 10^{-3}$  increased to  $X_i = 7.80 \times 10^{-3}$  after heating to 780°C (measured at room temperature). The  $X_i$ - $T$  curve of magnetic fraction is shown in Fig. 8f. The  $X_i$  hardly increased between room temperature and 450°C, and decreased through a maximum at 520°C,  $\Theta_{X_i}$  at 580°, and  $\Theta_{X_i}$  at 730°C on the heating curve. On the cooling curve the  $X_i$  increased between  $\Theta_{X_i}$  at 630°C and 400°C through a minor transition point,  $\Theta_{X_i}$ , at 580°C; and then decreased slightly on continued cooling. The properties of  $X_i$  of the bulk sample and the magnetic fraction did not correspond to each other.

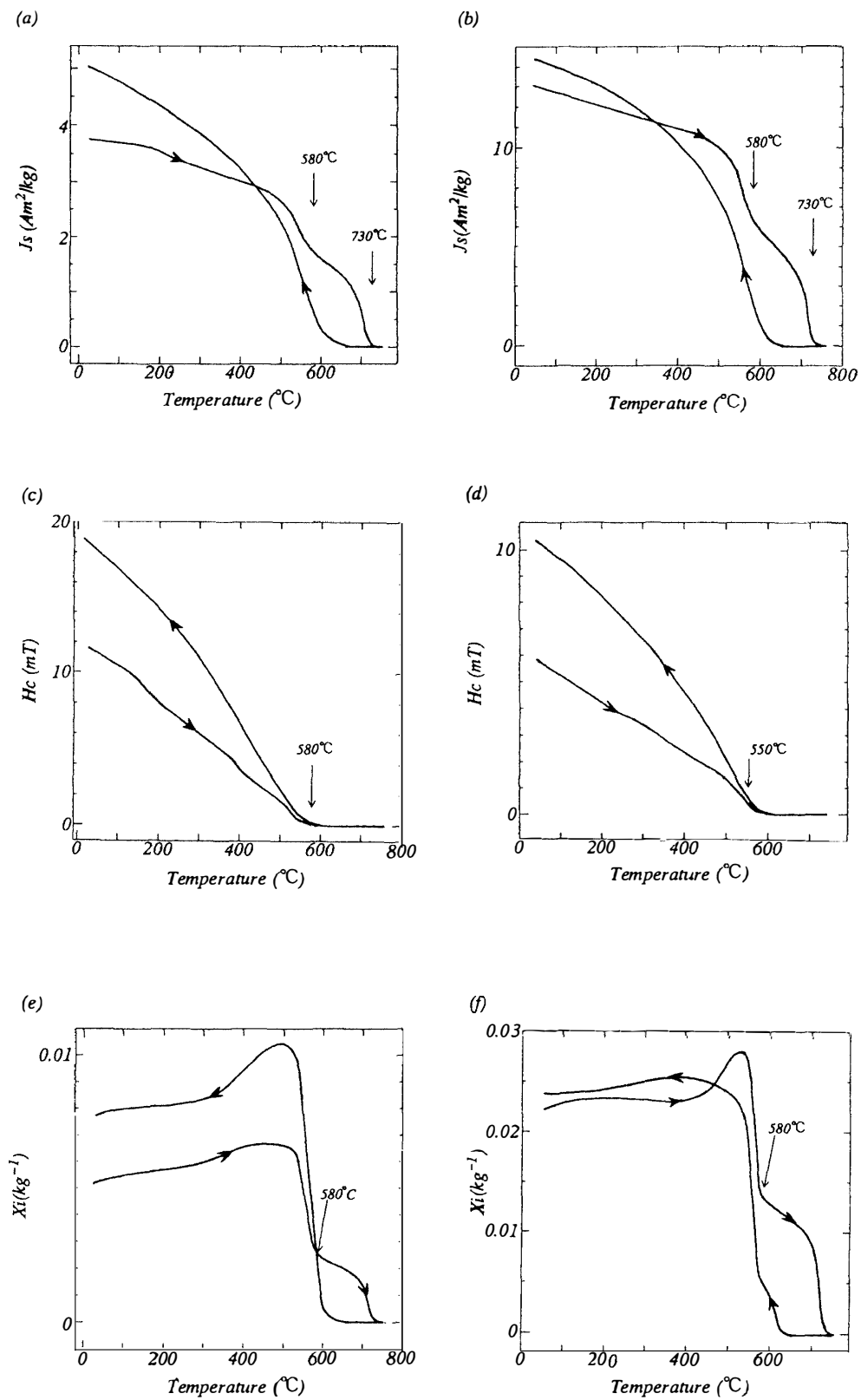


Fig. 8. Temperature dependence of  $J_s$ ,  $H_c$ ,  $X_i$  values for Willard chondrite. (a)(c)(e):  $J_s$ ,  $H_c$ ,  $X_i$  of the bulk sample. (b)(d)(f):  $J_s$ ,  $H_c$ ,  $X_i$  of the magnetic fraction (powder).

### 3.3.2. Natural remanent magnetization

NRM directions of eight small cubes obtained from Willard were scattered (Fig. 9). The results of thermal demagnetization, in steps of 50°C from 180° to 630°C, are shown in Fig. 10a. The NRM characteristics against thermal demagnetization showed a tendency for the NRM to be unblocked above 580°C corresponding to the disappearance of coercivity (Fig. 8c) although the intensity changes were less uniform than the other samples discussed in this paper. It seems that the main NRM carrier of the Willard meteorite is taenite and the contribution of abundant kamacite to Willard's NRM is small. The changes of directions of the residual NRM, plotted in Fig. 10a2, showed instability.

The stability of NRM of the Willard meteorite was not uniform in the subsamples. Fig. 10b1 shows plots of intensities of residual NRM against AF demagnetization up to 50 mT. The most stable NRM decayed to about 50% of the original NRM at 50 mT and the most unstable one decayed to 10% by 15 mT. One subsample showed a stable NRM (Fig. 10b2). The NRM seems to consist of two components (except the IRM, added to the original NRM, removed at 5 mT); the lower coercivity component dominated the coercivity range of 0 to 10 mT, and the higher coercivity component the range from 10 or 15 mT. The coercivity carried by magnetic grains in Willard does not seem to be distributed uniformly.

## 3.4. Forrest (b)

### 3.4.1. Thermomagnetic analysis

The  $J_s$ - $T$  curve of the bulk sample of the Forrest meteorite (shown in Fig. 11a) showed  $\Theta_{J_s}$  at 590°C and  $\Theta_{J_s}$  at 760°C on the heating curve and the  $\Theta_{J_s}$  at 580°C on the cooling curve. The heating curve is almost identical to the cooling curve between room temperature and  $\Theta_{J_s}$  at 580°C although the Ni composition of the taenite was almost the same as those in Tenham and Willard. The original  $J_s=5.86$  Am<sup>2</sup>/kg increased slightly to 6.21 Am<sup>2</sup>/kg (measured at room temperature) after heating to 780°C (Table 1). In the magnetic fraction obtained from Forrest, by hand magnetic separation, the  $J_s=2.16 \times 10$  Am<sup>2</sup>/kg increased to  $J_s=2.70 \times 10$  Am<sup>2</sup>/kg (Table 1). The heating  $J_s$ - $T$  curve of the magnetic fraction (Fig. 11b) showed two apparent  $\Theta_{J_s}$ s, at

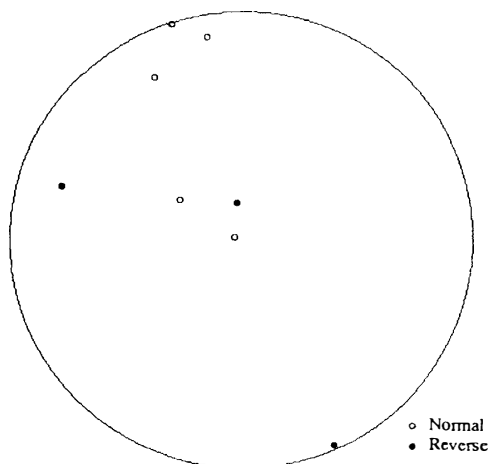


Fig. 9. NRM directions of eight small cubes of Willard.

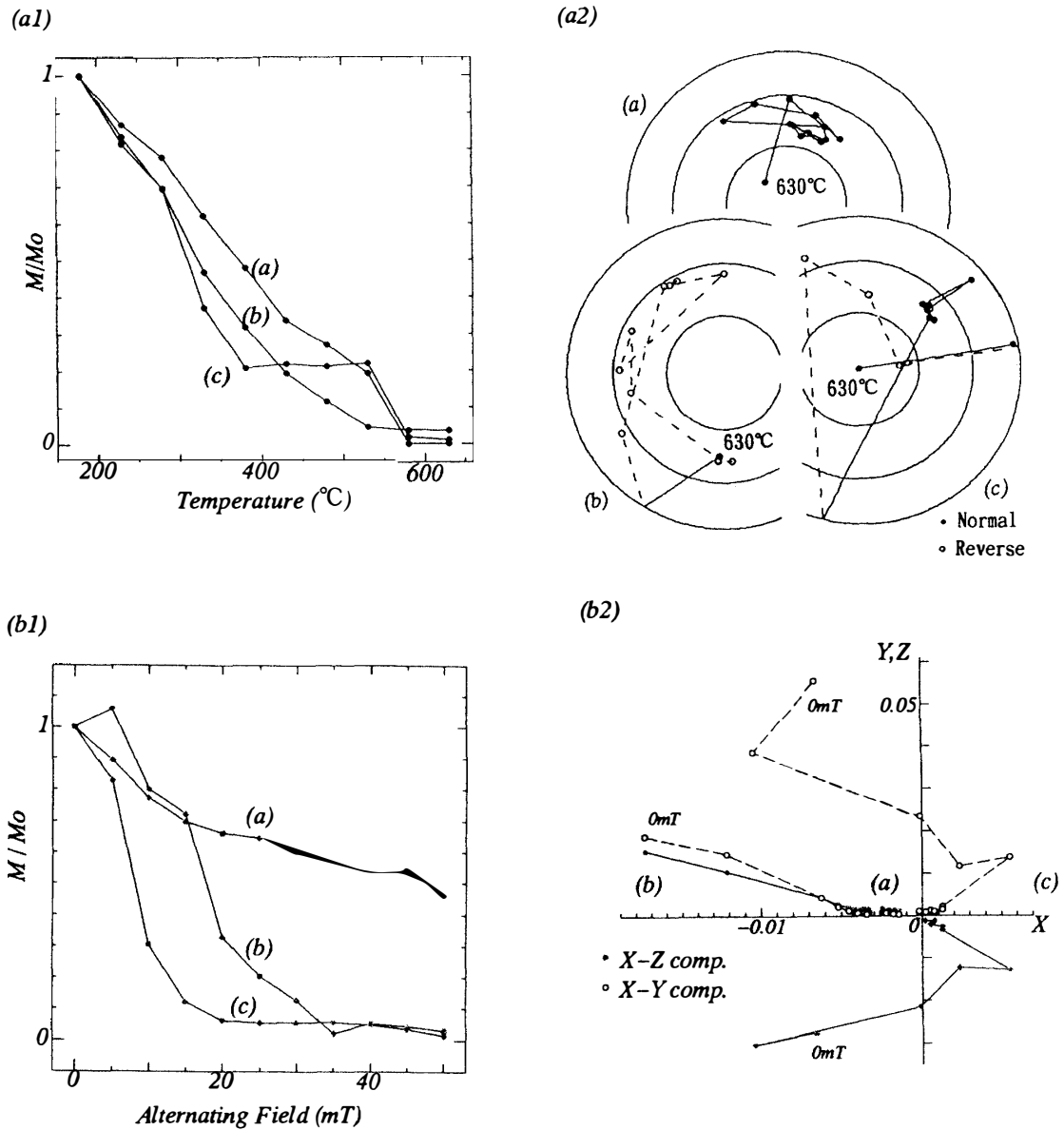


Fig. 10. Characteristics of NRM of Willard against thermal and AF demagnetization. (a1) Intensity changes against thermal demagnetization. (a2) Directional changes against thermal demagnetization. (b1) Intensity changes against AF demagnetization. (b2) Directional changes against AF demagnetization.

$560^{\circ}$  and at  $720^{\circ}\text{C}$ . The cooling curve showed two transition points,  $\Theta_{J_s}$ , at  $600^{\circ}$  and at  $520^{\circ}\text{C}$ . Main magnetic minerals in the Forrest meteorite are taenite with 54 at% Ni, on average, ( $\Theta_{J_s}$  at  $560^{\circ}$ – $590^{\circ}\text{C}$  as the apparent Curie point) and kamacite with 6 at% Ni, on average, ( $\Theta_{J_s}$  at  $720^{\circ}$ – $760^{\circ}\text{C}$  as the  $\alpha$ - $\gamma$  transformation temperature).

The  $H_c$ - $T$  curve of the bulk sample is shown in Fig. 11c. The coercivity had relatively high value and decreased gradually to an apparent  $\Theta_{H_c}$  at  $540^{\circ}\text{C}$  on the heating curve. On the cooling curve the coercivity increased gradually with an apparent  $\Theta_{H_c}$  at  $580^{\circ}\text{C}$  and minor ones at  $540^{\circ}$  and  $340^{\circ}\text{C}$ . The original  $H_c=23.80\text{ mT}$

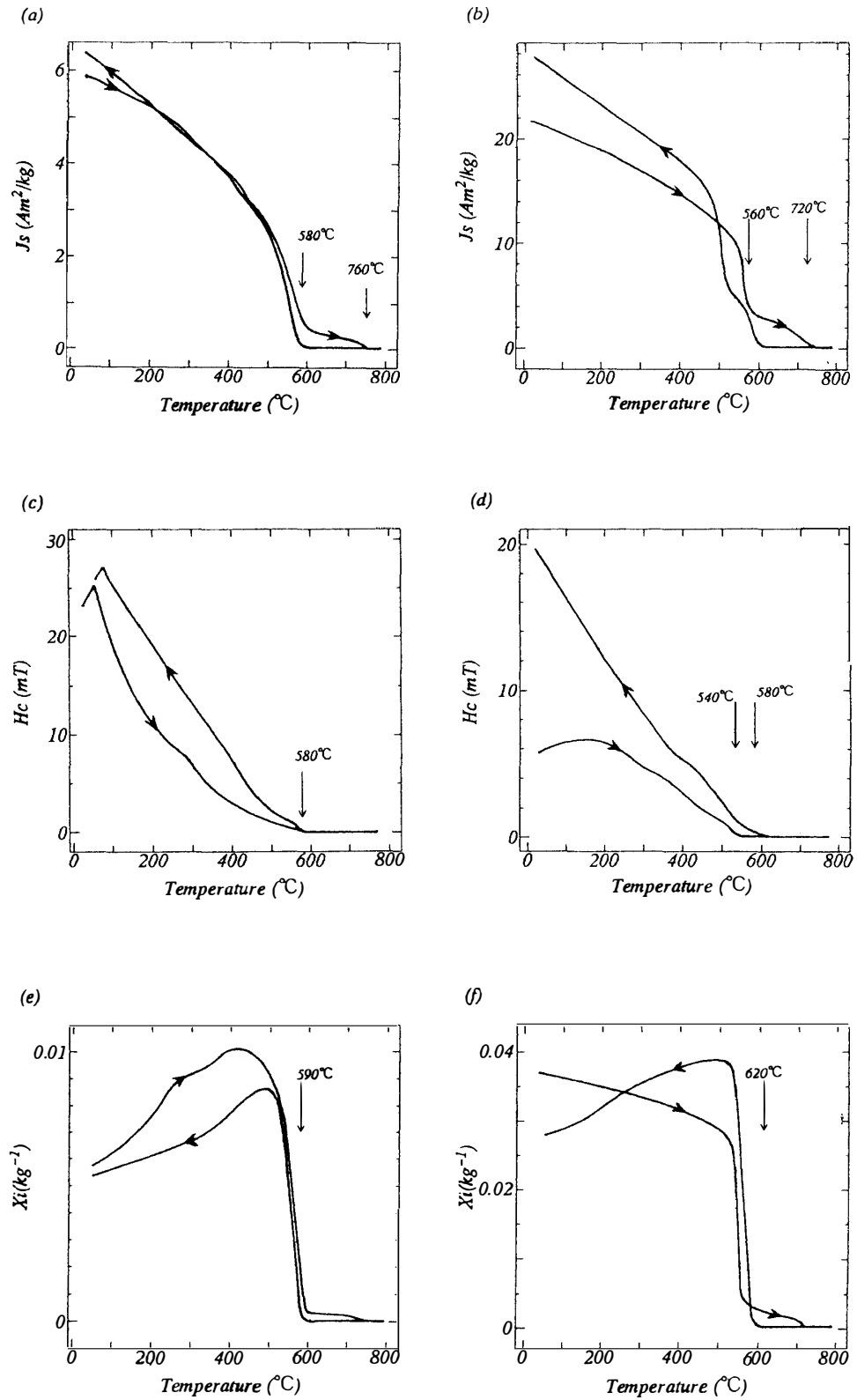


Fig. 11. Temperature dependence of  $J_s$ ,  $H_c$ ,  $X_i$  values for Forrest chondrite. (a)(c)(e):  $J_s$ ,  $H_c$ ,  $X_i$  of the bulk sample. (b)(d)(f):  $J_s$ ,  $H_c$ ,  $X_i$  of the magnetic fraction (powder).

slightly increased to  $H_c=25.24$  mT after heating to  $780^\circ\text{C}$  (measured at room temperature) (Table 1). The  $H_c$  of the magnetic fraction, before heating, was smaller than that of the pre-heating bulk sample (Fig. 11d). The  $H_c$ - $T$  curve showed  $\Theta_{H_c}$  at  $540^\circ\text{C}$  and  $410^\circ\text{C}$  on the heating curve and  $\Theta_{H_c}$  at  $580^\circ\text{C}$  and  $350^\circ\text{C}$  on the cooling curve. The pre-heating  $H_c=6.40$  mT increased to  $H_c=19.72$  mT after heating to  $780^\circ\text{C}$  (Table 1).

The  $X_i$ - $T$  curve of the bulk sample (Fig. 11e) gradually increased to  $440^\circ\text{C}$  and decreased abruptly between  $440^\circ\text{C}$  and the  $\Theta_{X_i}$  at  $600^\circ\text{C}$ , then reached almost to 0 at  $\Theta_{X_i}$  of  $760^\circ\text{C}$  on the heating curve. The cooling curve of the  $X_i$ - $T$  showed the  $\Theta_{X_i}$  at  $580^\circ\text{C}$  and the maximum at  $500^\circ\text{C}$  and gradual decreased during cooling. The original  $X_i=5.87\times 10^{-3}$  increased to  $X_i=7.84\times 10^{-3}$  after heat treatment (Table 1). The result of  $X_i$ - $T$  of the magnetic fraction is shown in Fig. 11f. The  $X_i$  decreased gradually to  $500^\circ\text{C}$  and abruptly between  $500^\circ\text{C}$  and  $\Theta_{X_i}$  at  $580^\circ\text{C}$ , then reached to the scale of 0 through the  $\Theta_{X_i}$  at  $720^\circ\text{C}$  on the heating curve. The cooling  $X_i$ - $T$  curve showed the  $\Theta_{X_i}$  at  $620^\circ\text{C}$  and a maximum at  $500^\circ\text{C}$ . The pre-heating  $X_i=3.79\times 10^{-2}$  of the magnetic fraction decreased to  $3.09\times 10^{-2}$  (at room temperature) after heating to  $780^\circ\text{C}$ .

#### 3.4.2. Natural remanent magnetization

NRM directions of eight small cubes obtained from Forrest were not completely random but were distributed on a hemisphere (Fig. 12). The NRM of the Forrest meteorite was thermally demagnetized, in steps of  $50^\circ\text{C}$ , from  $180^\circ$  to  $630^\circ\text{C}$ ; the results are shown in Fig. 13a. The directional changes of residual NRM were random but distributed on a hemisphere among the temperature change between  $180^\circ$  and  $580^\circ\text{C}$  steps (Fig. 13a2). The behavior of NRM, of Forrest, against thermal demagnetization was fairly unstable, not only in intensity but also in direction. The NRM of Forrest was quite unstable in its intensity and direction against AF demagnetization up to 50 mT (Fig. 13b).

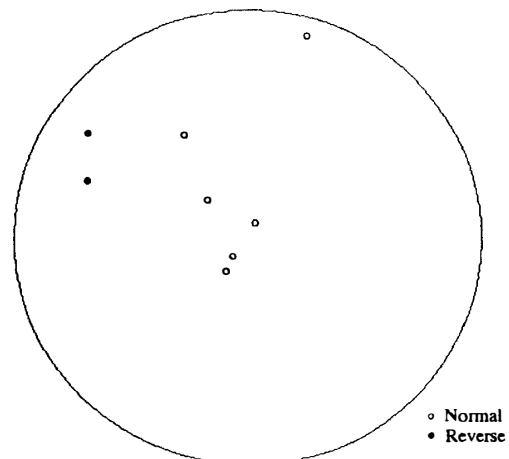


Fig. 12. NRM directions of eight small cubes of Forrest.

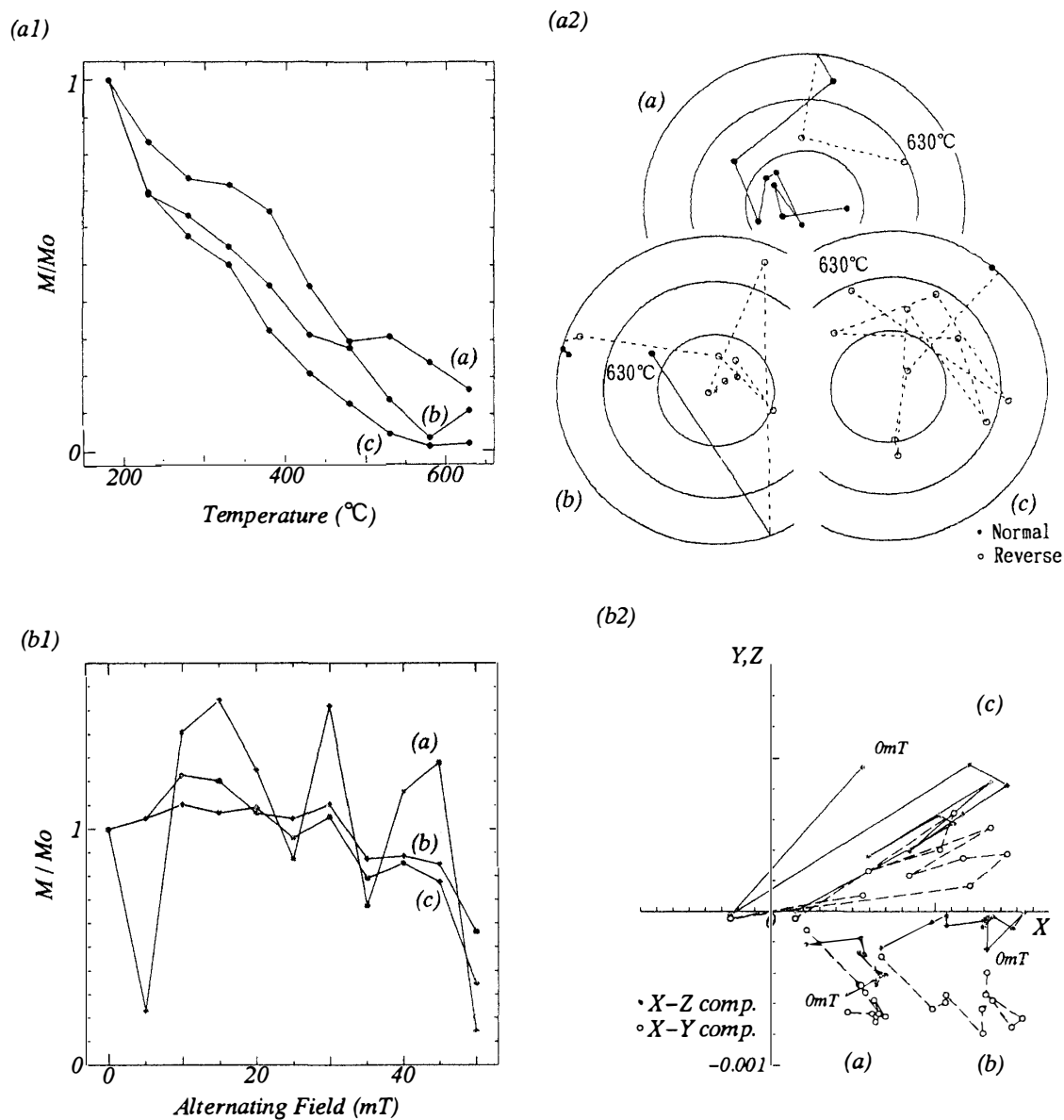


Fig. 13. Characteristics of NRM of Forrest against thermal and AF demagnetization. (a1) Intensity changes against thermal demagnetization. (a2) Directional changes against thermal demagnetization. (b1) Intensity changes against AF demagnetization. (b2) Directional changes against AF demagnetization.

#### 4. Discussion

The main magnetic minerals of the Tenham meteorite are taenite with 54 at% Ni and kamacite with 6 at% Ni on average. This composition of Tenham is similar to that of Willard with taenite having 54 at% Ni and kamacite with 7 at% Ni. In the present study, magnetic properties of Tenham and Willard do not satisfy the criteria reported by NAGATA and FUNAKI (1987) for a meteorite containing tetrataenite or  $\gamma'$ -(Fe, Ni). The magnetic criteria derived by them are summarized as follows: (1)  $H_{rc} \geq 50$  mT,

(2) the apparent Curie point is 560°–580°C, (3) the initial heating thermomagnetic curve of the  $\gamma'$ -phase is flat below about 500°C and then sharply drops at the apparent Curie point, (4) after heating above 700°C, the  $\gamma'$ -phase breaks down to the ordinary  $\gamma$ -phase, so that the cooling thermomagnetic curve has the characteristics of those of  $\gamma$ -phase, (5) because of the breakdown of the  $\gamma'$ -phase,  $H_c$  (and  $H_{rc}$ ) are much reduced from their pre-heating initial values. The flat curves of the initial heating  $J_s$ - $T$  curves of the Tenham and the Willard seem to show the non-saturated characteristics of  $\gamma'$ -phase and satisfy criteria (3) and (4), but the small original  $H_c$  and the increase after heating do not satisfy the criteria (5). And their  $H_c$ - $T$  properties were not identical to the cases of meteorites containing tetrataenite (FUNAKI, 1993). The tetrataenite seems to be absent or present in a negligibly small quantity in Tenham and Willard, in this study. It seems that the main NRM carrier is taenite and the contribution of abundant kamacite to the NRM is quite low in both Tenham and Willard, but their NRMs have quite different characteristics. The NRM of Tenham is stable and the NRM directions are relatively well grouped. That of Willard is more unstable and the NRM directions are very scattered. The coercivity of Tenham in the hysteresis loop examined in the magnetic field up to  $\pm 1$  T had a small value of 3.45 mT although the NRM was stable against the alternating field up to 50 mT. This would suggest that Tenham had acquired the stable NRM in its parent body without thermal blocking. On the other hand, the NRM of Willard is relatively unstable and showed varying response against both thermal and AF demagnetization. This may reflect heterogeneous distribution of magnetic minerals. It seems that Willard had not acquired the NRM in a stable magnetic field condition during its cooling process.

In the present study, the existence of tetrataenite in Tuxtuac was detected from the characteristics of coercivity during heating. But the powder sample of the magnetic fraction obtained by hand magnetic separation showed only very slight evidence of tetrataenite. In Fig. 5b the increase in coercivity of the powder sample of the magnetic fraction during heating seems to be due to the oxidation of sulfide and FeOOH left within the powder sample. The magnetic coercivity of a mixture of a magnetically hard component (having a large coercivity) and a soft component (having a small coercivity) is affected more extensively by the soft component than the hard component (NAGATA and FUNAKI, 1982). The value of  $H_c=37.78$  mT seems to reflect the existence of the tetrataenite similar to the cases of Y-74160 and Appley Bridge containing tetrataenite (NAGATA and FUNAKI, 1987). The tetrataenite seems to contribute to the NRM of Tuxtuac on the basis of the peculiar characteristics of the magnetization (or NRM) against heating similar to that of the tetrataenite lamellae obtained from Toluca iron (FUNAKI *et al.*, 1986). But the NRM of Tuxtuac was soft and mostly demagnetized by an alternating field up to 20 mT (Fig. 7b) although the NRM of tetrataenite lamellae of Toluca was very stable. This suggests that the NRM carried by Tuxtuac is softer than the IRM acquired in the magnetic field at 1 T. This hardly suggests that Tuxtuac had acquired the NRM (it must be of thermo-chemical origin, SUGIURA and STRANGWAY, 1982, because of formation of the tetrataenite, NAGAHARA, 1980) in the parent body with a stable magnetic field.

The main magnetic minerals of Forrest meteorite are taenite with 54 at% Ni and kamacite with 6 at% Ni, on average. The  $J_s$ - $T$  curve (Fig. 11a) of Forrest showed

almost reversible characteristics between room temperature and the Curie point of taenite. This characteristic of the saturation magnetization of Forrest did not correspond of those of Tenham and Willard in spite of the similarity of the Ni composition of the taenite in Tenham, Willard and Forrest. This would suggest that Forrest has experienced alteration in terrestrial environment. The NRM of Forrest was very unstable against both thermal and AF demagnetization. A secondary magnetization possibly due to terrestrial weathering seems to be added to the original NRM.

### 5. Summary

In this study, magnetic properties of Tenham, Tuxtuac, Willard and Forrest chondrites with or without the tetrataenite phase were examined and their NRM's were examined on the basis of the magnetic properties.

The main magnetic minerals of the Tenham are kamacite and taenite. The Tenham chondrite has stable NRM carried mainly by taenite, but the high value of coercivity expected from the stability to AF demagnetization is not satisfied by the magnetocrystalline anisotropy of the taenite ( $K_1 \approx 8 \times 10^2 \text{ J/m}^3$ , BOZORTH and WALKER, 1953).

The Tuxtuac chondrite contains tetrataenite and taenite, but carries a soft NRM in spite of its high coercivity. The tetrataenite, at least, had not acquired the CRM during cooling in its parent body. It suggests that the parent body of Tuxtuac had not possessed a significant magnetic field at least during the formation of the tetrataenite.

The main magnetic minerals of the Willard chondrite are kamacite and taenite and are similar to those in Tenham. Willard carries an unstable NRM mainly due to the taenite. In comparison to Tenham, Willard does not seem to have acquired stable NRM (or TRM) in its parent body during the cooling process.

The Forrest chondrite has experienced terrestrial alteration, the terrestrial NRM being added to the original NRM.

### Acknowledgments

We would like to thank Dr. N. SUGIURA of the University of Tokyo for his valuable and helpful comments.

### References

- ALBERTSEN, J. F., JENSEN, G. B. and KNUDSEN, J. M. (1978): Structure of taenite in two iron meteorites. *Nature*, **273**, 453–454.
- BOZORTH, R. M. and WALKER, J. G. (1953): Magnetic crystal anisotropy and magnetostriction of iron-nickel alloys. *Phys. Rev.* **89**, 624–628.
- FUNAKI, M. (1993): Temperature dependence of coercivity for chondrites. Allende, Allan Hills-769, and Nuevo Mercurio. *Proc. NIPR Symp. Antarct. Meteorites*, **6**, 391–400.
- FUNAKI, M., NAGATA, T. and DANON, J. (1986): Magnetic properties of lamellar tetrataenite in Toluca iron meteorite. *Mem. Natl Inst. Polar Res., Spec. Issue*, **41**, 382–393.
- NAGAHARA, H. (1980): Petrological study of Ni-Fe metal in some ordinary chondrites. *Mem. Natl Inst. Polar Res., Spec. Issue*, **17**, 111–122.

- NAGATA, T. and FUNAKI, M. (1982): Magnetic properties of tetrataenite-rich stony meteorites. Mem. Natl Inst. Polar Res., Spec. Issue, **25**, 222–250.
- NAGATA, T. and FUNAKI, M. (1987): Tetrataenite phase in Antarctic meteorites. Mem. Natl Inst. Polar Res., Spec. Issue, **46**, 245–262.
- NAGATA, T., FUNAKI, M. and DANON, J. (1986): Magnetic properties of tetrataenite-rich meteorites. Mem. Natl Inst. Polar Res., Spec. Issue, **41**, 364–381.
- NAGATA, T., DANON, J. and FUNAKI, M. (1987): Magnetic properties of Ni-rich iron meteorites. Mem. Natl Inst. Polar Res., Spec. Issue, **46**, 263–282.
- NÉEL, L., PAULEVE, J., PAUTHENET, R., LAUGIER, J. and DAUTREPPE, D. (1964): Magnetic properties of an iron-nickel single crystal ordered by neutron bombardment. J. Appl. Phys., **33**, 873–876.
- SCORZELLI, R.J. and DANON, J. (1985): Mössbauer spectroscopy and X-ray diffraction studies of Fe-Ni order-disorder in a 35% Ni meteorite (Santa Catharina). Phys. Scrip., **32**, 143–148.
- SUGIURA, N. and STRANGWAY, D. W. (1982): Magnetic properties of low-petrologic grade non-carbonaceous chondrites. Mem. Natl Inst. Polar Res., Spec. Issue, **25**, 260–280.
- WASILEWSKI, P. (1982): Magnetic characterization of tetrataenite and its role in the magnetization of meteorite. Lunar and Planetary Science X. Houston, Lunar Planet. Inst., 843–844.
- WASILEWSKI, P. (1985): Disordering of tetrataenite—the most significant magnetic mineral in the chondrite meteorites (abstract). EOS, **66**, 296.

*(Received August 1, 1994; Revised manuscript received November 12, 1994)*